Design Proposal: Mach-Zehnder Interferometers

ELAHEH KAROOBY*

Department of Electrical and Computer Engineering, North Carolina State University, Raleigh, North Carolina 27695, USA

** ekaroob@ncsu.edu*

Abstract: This report presents several configurations of Mach-Zehnder interferometers (MZIs) implemented on a silicon-on-insulator (SOI) platform. The proposed designs feature varying optical path length differences, alternative components and labeling schemes for the laser input. Design decisions are justified through a combination of analytical modeling and numerical simulations. The first version of the layout mask is provided for fabrication and automated testing at UBC, comprising four TE-polarized MZIs integrated withing a 605 μm × 420 μm chip area.

1. Introduction

Mach–Zehnder interferometers (MZIs) are fundamental components in integrated photonics, widely used to translate relative phase differences between two optical paths into measurable intensity variations at the output [1]. Due to this property, MZIs serve as core building blocks for devices such as optical modulators, switches, sensors, and signal processors [2,3]. Silicon-on-insulator (SOI) technology provides a particularly attractive platform for MZI implementation, offering high refractive index contrast, compact device footprints, and compatibility with CMOS fabrication processes [4].

This report is organized as follows. Section 2 presents the theoretical background of the MZI transfer function. Section 3 describes the waveguide design and MZI modeling and analysis. Section 4 introduces 2nd version of the layout prepared for fabrication and automated testing. Finally, Section 5 summarizes the main results and conclusions.

2. Theory

To find the transfer function of an MZI with a Y-branch beam splitter we consider an input intensity of I_i corresponding to an electric field, E_i. The intensity of light at each of the beam splitter outputs is $I_1 = I_2 = I_i/2$, corresponding to the electric fields $E_1 = E_2 = E_i/\sqrt{2}$. The second beam splitter which operates as a combinere provides the fundamenral mode and the radation modes. The electric field at the output of the combiner is $E_{o1} = E_1/\sqrt{2}$ or $E_{o2} = E_2/\sqrt{2}$. Therefore, the output field is $E_o = E_1 + E_2/\sqrt{2}$. For a plane wave with apropagation constant of $\beta = \frac{2\pi n}{\lambda}$, assuming no loss:

$$E_{o1} = E_1 e^{-j\beta L_1} = \frac{E_i}{\sqrt{2}} e^{-j\beta L_1} \quad (1)$$

$$E_{o2} = E_2 e^{-j\beta L_2} = \frac{E_i}{\sqrt{2}} e^{-j\beta L_2} \quad (2)$$

Therefore, the output electric field of the y-branch is

$$E_o = \frac{E_{o1}+E_{o2}}{\sqrt{2}} = \frac{E_i}{2}(e^{-j\beta L_1} + e^{-j\beta L_2}) \quad (3)$$

The intensity is

$$I_o = \frac{I_i}{4}(e^{-j\beta L_1} + e^{-j\beta L_2})^2 = \frac{I_i}{2}(1 + \cos(\beta \Delta L)) \quad (4)$$

Hence, the transfer function of the MZI is

$$T_{MZI}(\lambda) = = \frac{I_i}{2}(1 + \cos(\beta \Delta L)) \quad (5)$$

3. Modeling and Simulation

3.1 Waveguide Modeling and Anaysis

We designed Si strip waveguides with a $220nm$ height, and $500nm$ width to support fundamental TE mode at wavelength of 1550 nm. We used Lumerical FDE simulation tool for numerical analysis. In the simulation, Si waveguides are surrounded by SiO_2 BOX and cladding, as illustarted in Fig. 1.

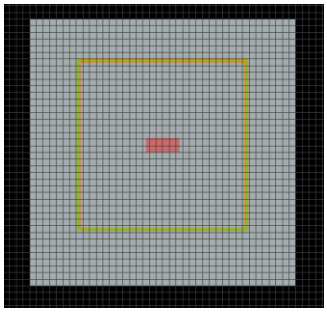

Fig. 1 Top view of a Si strip waveguide (red rectangle) surrounded by SiO_2 BOX and cladding (gray square). The yellow square border shows the simulation region.

Figure 2 illustrates the intensity of electric field (Fig. 2(a)) and the E_x componenet Fig. 2(b)). As expected from the boundary conditions in Maxwell's equations, we see the discontinuities in the Electric field at the SiO_2 interface.

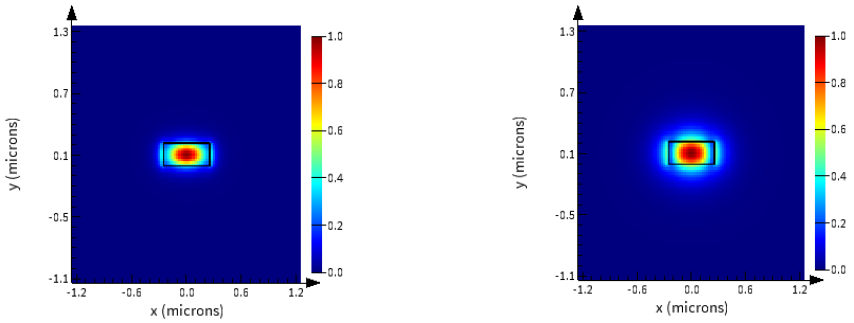

Fig. 2 Quasi-TE mode profile: (a) electric filed intensity, (b) E_x component.

Figure 3(a) illustrates the effective index, and Fig. 3(b) shows the group index of the waveguide for the fundamental quasi-TE mode. As the wavelength increases, the effective index decreases, whereas the group index exhibits an increasing trend.

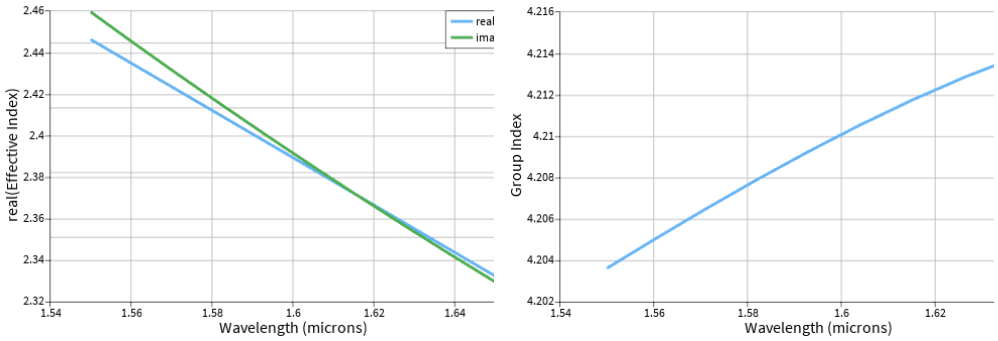

Fig. 3 Quasi-TE mode profile: (a) electric filed intensity, (b) E_x component.

The compact model of the waveguide is a second order polynomial. We can use a Taylor expansion around the center wavelength, of the form:

$$n_{eff}(\lambda) = n_1 + n_2(\lambda - \lambda_0) + n_3(\lambda - \lambda_0)^2 \qquad (6)$$

We use the simulated data as the input matrix for the fitting algorithm and then find the expression that correctly describes the waveguide. The Taylor expansion parameters can also be converted to conventional parameters (effective index, group index, and dispersion) at the wavelength: $n_{eff} = n_1$, $n_g = n_1 - n_2.\lambda_0$, and D $= -2.\lambda_0.n_3/c$ [s/m^2]. After running the Lumerical mode simulations, we use the script provided at the end of this report and run it in the script prompt. to find the coefficients (n_1, n_2, n_3) for the Waveguide compact model.

$$n_{eff}(\lambda) = 2.446 - 1.134(\lambda - \lambda_0) - 0.035(\lambda - \lambda_0)^2 \qquad (7)$$

Figure 4 illustrates the compact model for the fundamental TE mode.

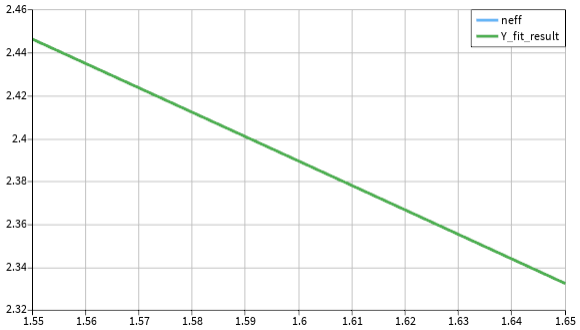

Fig. 4 The compact model for the fundamental TE mode

3.2 MZI Modeling and Analysis

Using equation 5, the free spectral range (FSR) of the MZI can be calculated as

$$FSR = \lambda^2/n_g\Delta L \qquad (8)$$

To study the effect of the path length difference ΔL on the FSR, we consider two MZIs: MZI1 with $\Delta L_1 = 50\mu m$ and MZI2 with $\Delta L_2 = 150\mu m$. The calculated FSR values are $11.44nm$

and $3.81nm$ respectively, showing that a longer optical path length difference results in a smaller FSR.

Figure 5 illustrates the spectra of MZI1 and MZI2 at the two output channels, Ch1 and Ch2. The simulated FSRs are $11.75nm$ for ΔL_1 and $3.79nm$ for ΔL_2, which are in good agreement with the calculated values. Table 1 lists the calculated and simulated FSR for MZI1 and MZI2.

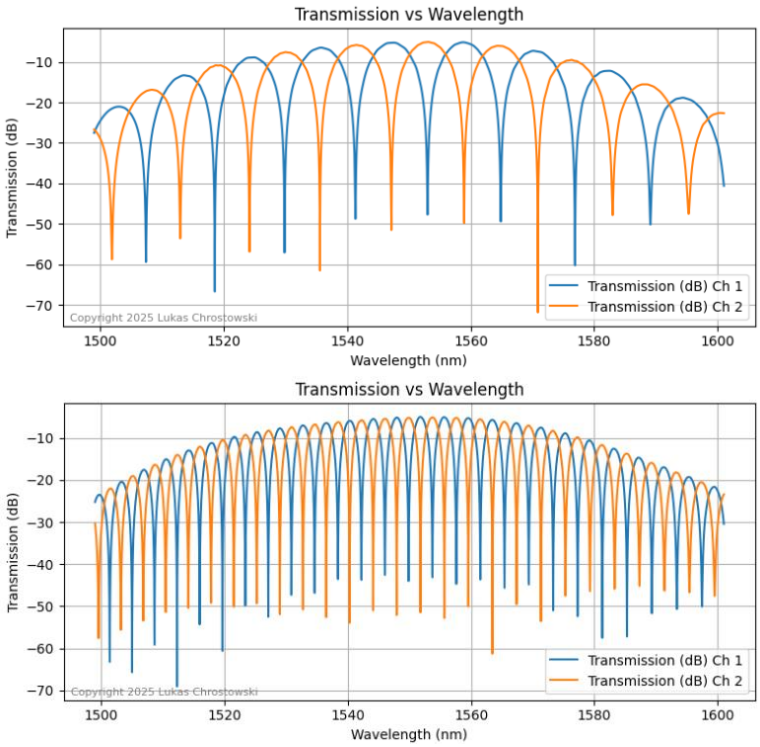

Fig . 5 The spectrum of (a) MZI1 with $\Delta L_1 = 50\mu m$, and (b) MZI2 with $\Delta L_2 = 150\mu m$.

Table 1. Calculated and simulated FSR for MZI1 and MZI2

Circuit	$\Delta L(\mu m)$	Calculated FSR (nm)	Simulated FSR
MZI1	50.057	11.44	11.75
MZI2	150.015	3.81	3.79

To investigate alternative components and labeling schemes for the laser input, we consider MZI3 and MZI4. While MZI1 and MZI2 are consisting of one y-branch, one bidirectional coupler, and three grating couplers (one laser input, two output channels), MZI3 and MZI4 consist of two bidirectional couplers, and therefore four grating couplers (one laser input, three output channels). For MZI1 and MZI2, the laser input is the first grating coupler on top, while for the MZI3 and MZI4, the laser input is on the second grating coupler to facilitate the automated testing. MZI3 and MZI4 have the optical path length difference of $\Delta L_3 = 50nm$ and $\Delta L_4 = 150nm$,respectively. Since the FSRs of MZI3 is the same as that of MZI1, and the FSR of MZI4 is the same as that of MZI2, due to their identical path length differences, they are not included in table 1.

Figure 6 shows the spectra of MZI1 and MZI2 at the three output channels, Ch1, Ch2, and Ch3. MZI3 and MZI1 exhibit similar spectral responses since both have a path length difference of 50 nm, despite differences in component layout and laser input labeling. Similarly, MZI4 and MZI2 display comparable spectra for the same reason.

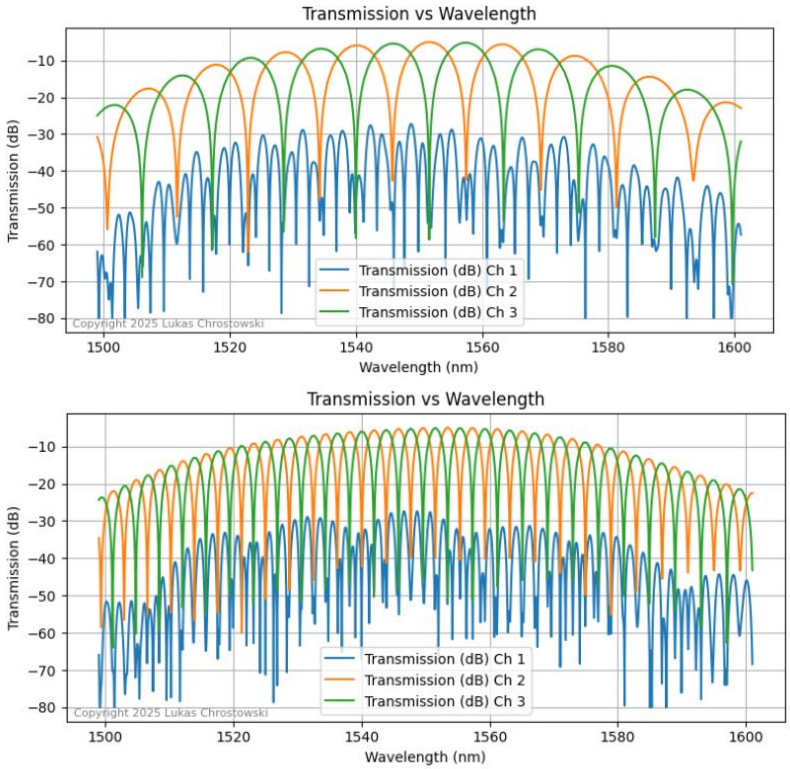

Fig . 6 The spectrum of (a) MZI3 with $\Delta L_1 = 50nm$, and (b) MZI4 with $\Delta L_2 = 150nm$.

Finally, we consider two de-embedding structures by replacing all devices (except grating couplers) with a waveguide. The purpose of this is that we can use this structure as a baseline for the loss of the more complicated structure. This lets us isolate just the devices we care about characterizing. Each de-embedding structure consists of two TE grating couplers connected by a TE waveguide, with a different connecting waveguide length for each structure. The gain for both de-embedding structures are the same and shown in Fig. 7.

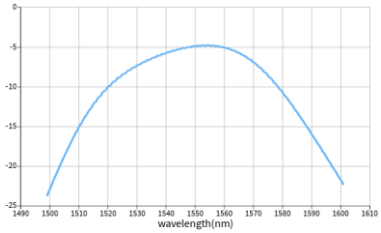

Fig . 7 TE gain (db) for the de-embedding structures.

4. Layout

The 2nd version of the layout for fabrication is illustarted in Fig. 8.

The circuits show MZI1 to MZI4, and two de-embedding structures, from left to right. Table 2 provides the details of each circuit.

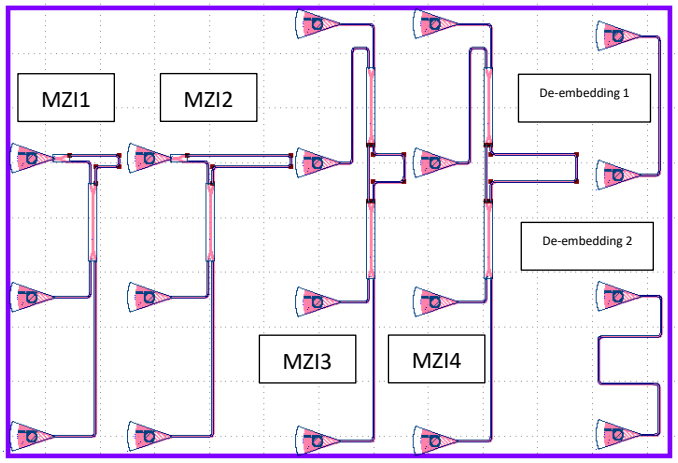

Fig . 8 The 2nd version of layout for fabrication.

Table 2. List of componenets used in the circuits

Circuit	Bidirectional couplers/Y-branch	Grating couplers	ΔL	Input	Output
MZI1	1/1	3	50.057	1st grating coupler from top	Ch1, Ch2
MZI2	1/1	3	150.015	1st grating coupler from top	Ch1, Ch2
MZI3	2/0	4	50.031	2nd grating couplers from top	Ch1, Ch2, Ch3
MZI4	2/0	4	150.019	2nd grating couplers from top	Ch1, Ch2, Ch3
De-embedding1	0	2	-	1st grating coupler from top	Ch1
De-embedding2	0	2	-	1st grating coupler from top	Ch1

5. Summary

In this report, we designed four MZIs supporting Fundamental Quasi-TE mode to study the effect of various optical path length differences, different couplers, and various laser input labeling on the spectra. We have also shown the loss of the grating couplers by including two

de-embedding structures in our layout. The simulation results are in great agreement with theoretical calculations and analysis.

References

1. B. E. A. Saleh and M. C. Teich, *Fundamentals of Photonics*, 2nd ed. (Wiley, 2007).

2. G. T. Reed, G. Mashanovich, F. Y. Gardes, and D. J. Thomson, "Silicon optical modulators," Nature Photonics 2010 4:8 **4**(8), 518–526 (2010).

3. J. Leuthold, C. Koos, and W. Freude, "Nonlinear silicon photonics," Nature Photonics 2010 4:8 **4**(8), 535–544 (2010).

4. D. Thomson, A. Zilkie, J. E. Bowers, T. Komljenovic, G. T. Reed, L. Vivien, D. Marris-Morini, E. Cassan, L. Virot, J. M. Fédéli, J. M. Hartmann, J. H. Schmid, D. X. Xu, F. Boeuf, P. O'Brien, G. Z. Mashanovich, and M. Nedeljkovic, "Roadmap on silicon photonics," Journal of Optics **18**(7), 073003 (2016).

Script

```
# Get the data from the MODE frequency sweep

lambda=c/getdata("FDE::data::frequencysweep","f")*1e6; # lambda in [microns]

neff=abs(getdata("FDE::data::frequencysweep","neff"));

lambda0 = 1.55;  # central wavelength

# Polynomial fitting.

x_fit = lambda-lambda0; # X vector

y_fit = neff;          # Y vector

n_fit = 2;             # order of the polynomial

# Next 3 lines do polyfit. Inputs: x_fit, y_fit, n_fit. Outputs: a_fit.

# Based on a linear algebra approach

X_fit = matrix(length(x_fit),n_fit+1);

for(i_fit=0:n_fit){ X_fit(1:length(x_fit),i_fit+1) = x_fit^i_fit; }

a_fit = mult(mult(inv(mult(transpose(X_fit),X_fit)),transpose(X_fit)),y_fit);

# Display the fit polynomial coefficients

?a_fit;

# This is the polynomial equation:
```

Y_fit_result = a_fit(1) + a_fit(2)*(lambda-lambda0) + a_fit(3)*(lambda-lambda0)^2;

plot (lambda, neff, Y_fit_result); # plot the result

The results:

2.44623 (This is n_1 which is infact n_{eff})

-1.13422 (This is n_2)

-0.0355 (This is n_3)